



14th Deep Sea Offshore Wind R&D Conference, EERA DeepWind'2017, 18-20 January 2017, Trondheim, Norway

# Fatigue Crack Detection for Lifetime Extension of Monopile-based Offshore Wind Turbines

Jutta Stutzmann<sup>a,b,\*</sup>, Lisa Ziegler<sup>c,d</sup>, Michael Muskulus<sup>d</sup>

<sup>a</sup>University of Stuttgart, Stuttgart Wind Energy @ Institute of Aircraft Design, Allmandring 5B, 70569 Stuttgart, Germany

<sup>b</sup>Chalmers University of Technology, Maskingränd 2, 41258 Gothenburg, Sweden

<sup>c</sup>Rambøll, Stadtdeich 7, 20097 Hamburg, Germany

<sup>d</sup>Norwegian University of Science and Technology, Department of Civil and Environmental Engineering, Høgskoleringen 7a, 7491 Trondheim, Norway

---

## Abstract

Lifetime extension becomes increasingly crucial for industry, since the first offshore wind farms face the end of their design lifetime. The remaining useful lifetime of offshore foundations is driven by fatigue design and loading; both are affected by uncertainty. This paper presents a conditional probability model to link results from inspections with numerical simulations of fatigue cracks. Crack sizes are simulated with a fracture mechanics model applying Paris' Law. The probability of detection of an existing crack depends on inspection technique and crack size. Results show that uncertainty about remaining useful lifetime significantly reduces after considering inspection outcomes. This decreases risks for the decision-making on lifetime extension of offshore wind turbines.

© 2017 The Authors. Published by Elsevier Ltd.  
Peer-review under responsibility of SINTEF Energi AS.

**Keywords:** offshore wind energy; lifetime extension; remaining useful lifetime; fatigue crack propagation; crack detection; probability of detection; conditional probability; Bayesian analysis

---

## 1. Introduction

The operating life of offshore wind turbines (OWT) is limited to at least 20 years [1]. In the upcoming years the first wind farms reach the end of their planned service time. Lifetime extension of OWT is an option to save on investment and planning of new wind farms [2]. It would not only reduce costs and economize resources, but would also keep the environmental balance [2]. To address the question whether lifetime extension is feasible, the structural integrity of all wind turbine components must be assessed [3]. The remaining useful lifetime (RUL) of offshore wind support structures is driven by fatigue design and loading of the turbine [4,5]. Uncertainties in environmental, structural and operational conditions demand probabilistic assessment of fatigue cracks in the support structure. Fatigue crack

---

\* Corresponding author. Tel. 1: +45-52798370; Tel. 2: +49-160 8134855  
E-mail address: [jutta@stutzmann.de](mailto:jutta@stutzmann.de)

growth is highly sensitive to input parameter variations, like initial crack size [4]. Crack propagation can be analyzed by means of a fracture mechanics model applying Paris' Law [4].

To the knowledge of the authors, public information about lifetime extension in the industrial sector of OWTs is rare, although some scientific publications are available. Kallehave et al. [14] point out that monopiles can be eligible for a longer lifetime based on measurements of first natural frequencies. Reassessment of the fatigue lifetime was performed for monopile substructure of OWTs in [15]. Ziegler [16] suggests an approach on 'structural reassessment, predictions on RUL, and a decision model' focusing on offshore monopile-based structures.

DNV GL [1] recently released a standard for lifetime extension of wind turbines and a related specification on certification [6]. This standard recommends 'a twofold assessment' for lifetime extension. The 'analytical part' can be realized either by deterministic approaches (simplified or detailed) or stochastic methods. The 'practical part' includes a detailed inspection scope. To assess whether lifetime extension of OWTs is feasible, each structure has to be inspected individually.

Underwater inspection of OWT foundations with a focus on fatigue crack growth is discussed in [7]. This guideline presents 'the use of probabilistic methods for inspection planning of fatigue cracks in jacket structures, semisubmersibles and floating production vessels' [7]. May et al. [8] point out health and safety risks which stem from underwater inspection in Health and Safety Executive (HSE) books. Risks as well as costs are qualitatively stated by May et al. [8] and Bussi eres et al. [9]. The American Society of Non-destructive Testing (ASNT) [10] and the Non-destructive Testing (NDT) Education Research Centre [11] provide an overview about further feasible inspection techniques for fatigue crack detection at offshore structures. Specified recommendations for crack inspection of monopile-based offshore structures are neither included in the report by DNV GL [7] nor by others [8,10,11]. However, analogies to monopiles are assumed in this study, since monopiles show similarities to other offshore structures.

DNV GL gives recommendations on the probability of detection (PoD) of a fatigue crack for the most common non-destructive inspection techniques [7]. PoD depends on inspection technique and crack size and is afflicted with large uncertainties. To reduce uncertainties Moan [12] presents a theoretical approach for stochastic analyses. This method is based on a conditional probability analysis applying Bayes' Theorem. Crack size distributions from simulations are updated using detection outcomes from inspections and their PoD. Lotsberg et al. [13] shows updated crack size distributions after inspections for jacket structures in the oil and gas industry by means of conditional probability models.

The novelty of this study is to update simulated crack size distributions at monopile-based OWTs with detection results from underwater inspection. The used method follows the strategy recommended by Moan [12]. This approach implements conditional probability analysis by means of Bayes' Theorem. Thus, this study investigates whether crack inspections lower uncertainties in RUL predictions for OWTs. The paper is structured in the following way. Section 2 introduces the stochastic fatigue crack growth model. In Section 3 the conditional probability model applying Bayes' Theorem is presented. Predictions of crack size and RUL considering detection results are discussed in Section 4. A brief conclusion is provided in Section 5.

## Nomenclature

$a$	crack size = crack depth	$N$	number of cycles
$a_0$	initial crack size	$n$	time
$a_{fail}$	failure crack size	$P$	probability
$a_n$	crack size after $n$ years	$PoD$	probability of detection
$b$	distribution parameter	$S$	stress range
$B$	number of bins	$\bar{S}_k$	mean value in stress range $k$
$C$	crack growth parameter	$X_0$	distribution parameter
$K_j$	stress intensity factor	$Y$	geometry parameter
$m$	material constant	$z$	event of detection

## 2. Methodology

### 2.1. Fracture mechanics model

OWTs are highly dynamic systems exposed to cyclic loading from aero- and hydrodynamic excitation [17]. The design of support structures is often governed by fatigue constraints. Crack initiation, continuous crack propagation, and brittle failure are the phases of fatigue life of a structure [18]. Crack propagation is the dominant phase for welded structures and can be simulated with linear-elastic fracture mechanics models. Paris' Law, a simplified engineering model to describe fatigue crack propagation, is used in this study [19]. It describes the change of a crack size  $a$  over the number of load cycles  $dN$  as shown in Equation 1. This fraction equals the crack growth parameter  $C$  times the stress intensity factor  $\Delta K_j$  to the power of the material constant  $m$ .

$$\frac{da}{dN} = C(\Delta K_j)^m \quad (1)$$

$\Delta K_j$  is a function of the geometry factor  $Y$ , stress ranges  $\Delta S$  at the regarded hotspot (*here: mudline*), and the current crack size  $a$ .

$$\Delta K_j = \Delta S \cdot Y \sqrt{a\pi} \quad (2)$$

Paris' Law is applicable to fatigue cracks larger than a specified threshold that fulfill the conditions of linear-elastic fracture mechanics. Small cracks (crack initiation phase) interact with the microstructure of the material and are typically analysed with continuum mechanics approaches [20–22]. We assume in this study that the crack initiation phase has no influence on the fatigue life of monopile welds. All cracks - regardless of their initial size - are assumed to be in the crack propagation phase and are analysed with Paris' Law.

### 2.2. Stochastic crack propagation model

In this study a stochastic approach was performed to consider uncertainties in input parameters. Paris' Law (cf. Equation 1) was solved according to Kirkemo [23].

$$\psi(a_n) = \int_{a_0}^{a_n} \frac{da}{Y^m (\sqrt{a\pi})^m} \quad (3)$$

$$\psi(a_n) = CS^m \Delta N \quad (4)$$

The integration of Paris' Law in Equation 3 can be solved directly if the stress ranges  $S$  are constant. This is not applicable for OWTs which experience variable amplitude loading. Therefore, as a simplification, the stress ranges  $S$  of variable amplitudes are divided in  $k$  bins (*here: bin size = 1 MPa, total number of bins  $B = 67$* ). The mean value  $\bar{S}_k$  of each bin is the corresponding constant amplitude loading. The binning and integration ignores the sequence in which stress amplitudes occur in the structure. Previous work has shown that the sequence effect is very small for offshore wind monopiles and can be neglected [5].

By applying the numerical integration and rearranging Equation 3 and 4 the crack size after  $n$  years results in:

$$a_n = \left( a_0^{1-0.5m} - \frac{(m-2)}{2} \pi^{0.5m} C Y^m \sum_{k=1}^B \bar{S}_k (\Delta N)_k \right)^{\frac{1}{1-0.5m}} \quad (5)$$

Stress ranges  $S$  and the number of load cycles  $\Delta N$  used in this study were adapted from a previous project [5]. The simulation length was one hour for each loading scenario. Rainflow counting was performed on the resulting time series of stresses at mudline to obtain  $S$  and  $\Delta N$  [5]. Reference is made to Ziegler et al. [5] for further information on the numerical model and load simulations.

$a_0$  represents the initial crack size,  $a_n$  stands for the crack size after  $n$  years. For stochastic crack growth analysis distributions of initial crack size  $a_0$ , crack growth parameter  $C$ , and geometry factor  $Y$  were considered.  $C$  and  $m$

are dependent on each other and the material constant  $m$  was set to 3.1 as a model simplification [5,7,13]. Several offshore standards provide recommended values for input data based on experimental data [7,24,25]. The initial crack size distribution is assumed to follow an exponential progression with a mean value at 0.043 mm and median value at 0.030 mm [7,13]. Both, crack growth parameter and geometry factor are assumed as normal distributions [7]. Mean values and units are mentioned in Table 1 according to DNV GL [7]. Figure 1 - 3 illustrate the distributions of the stochastic input parameters.

To address the question of crack size distribution after  $n$  years a Monte Carlo simulation ( $10^6$  samples) was applied. Input values were chosen randomly out of their distributions as input to the simulation of fatigue crack growth over  $n$  years of design lifetime (*here:  $n = 20$* ). Subsequently, Equation 5 was applied to calculate RULs considering the failure crack size  $a_{fail}$  and simulated crack sizes  $a_n$  after 20 years. The critical crack size value  $a_{fail}$  was set to 60 mm, which equals the monopile wall thickness [5]. The simulation stopped when a crack reaches the size of 60 mm within the first 20 years of lifetime. Those results were neglected for further evaluations in this study. This assumption could be made, since the assessment was performed after 20 years of design lifetime. Therefore, RULs were only estimated for OWTs which have reached the 20 years already.

Table 1. Mean/median values and units of input parameters according to DNV GL [7].

Parameter	Mean value / Standard deviation	Unit
Initial crack size $a_0$	0.043 / 0.043	mm
Geometry factor $Y$	1 / 0.1	-
Crack growth parameter $C$	$3.322 \cdot 10^{-13}$ / $1.660 \cdot 10^{-13}$	$\frac{mm}{(MPa \sqrt{mm})^m}$

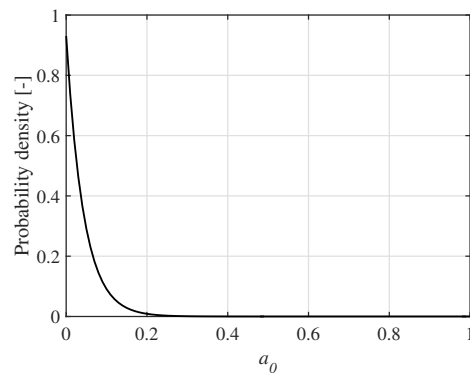


Fig. 1. Initial crack size  $a_0$  [mm]

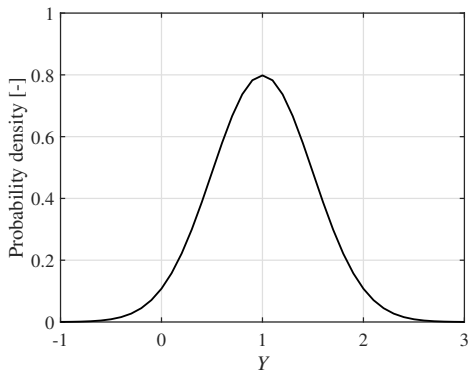


Fig. 2. Geometry factor  $Y$  [-]

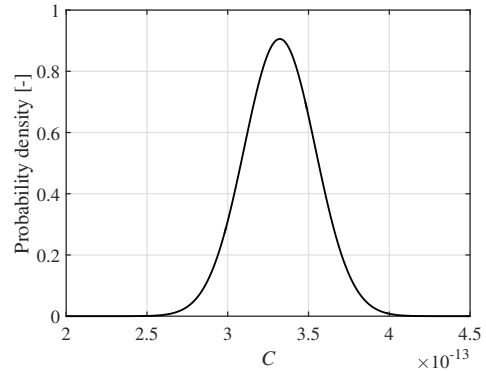


Fig. 3. Crack growth parameter  $C$   $\left[ \frac{mm}{(MPa \sqrt{mm})^m} \right]$

### 2.3. Probability of detection

The PoD shows how likely it is that a crack of size  $a$  will be detected during an inspection. The PoD depends on the inspection technique as well as on the crack size  $a$  and increases with bigger crack sizes. However, the choice of inspection technique is not only driven by the PoD value. The decision on whether a technology can be practically implemented depends also on health and safety issues as well as on costs and accessibility [8]. The most common non-destructive techniques according to DNV GL, ASNT, NDT, and May et al. [7,8,10,11] are:

- Eddy Current (EC),
- Magnetic Particle Inspection (MPI),
- Ultrasonic Testing (UT),
- Alternating Current Field Measurement (ACFM), and
- Visual inspection.

Equation 6 presents the PoD calculation for inspection techniques EC, MPI, ACFM, and UT. Distribution parameters  $b$  and  $X_0$  depend on inspection technique as well as on the access to the inspected part (cf. Table 2). Failures at parts with more difficult access and below water are less likely to be detected. The distribution parameters  $b$  and  $X_0$  for EC, MPI, and ACFM inspection are set as equal and there is no difference between easy and difficult access to the inspected part, according to DNV GL [7].

It should be noted that visual inspection is feasible for offshore crack detection [7,8,10,11]. Visual inspection has a low PoD, but can be integrated to support other techniques [7]. However, visual inspection is very expensive due to the risk involved for the diver.

$$PoD(a) = 1 - \frac{1}{1 + \left(\frac{a}{X_0}\right)^b} \quad (6)$$

Table 2. Distribution parameters according to DNV GL [7].

Distribution parameters	$b$	$X_0$
EC	0.900	1.160
MPI	0.900	1.160
ACFM	0.900	1.160
UT	0.642	0.410

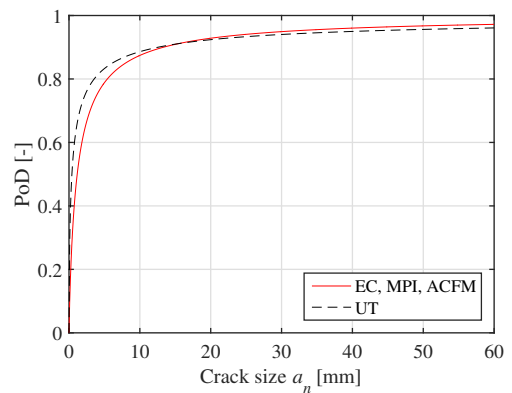


Fig. 4. PoD curve for ED, MPI, ACFM and UT

In this study crack size distribution is updated with the PoD from EC technique. According to Equation 6 and the distribution parameter  $b = 0.900$  and  $X_0 = 1.160$  (cf. Table 2) PoD is calculated individually for each simulated crack size value  $a_n$ .

### 3. Conditional Probability Model

To update crack size distributions with detection results a conditional probability model is required. In this study Bayes' Theorem was used to calculate the crack size distribution after inspection. Four different cases can occur:

- Case (i): crack exists and is detected,
- Case (ii): crack exists and is not detected ,
- Case (iii): crack does not exist and is detected (false alarm), and
- Case (iv): crack does not exist and is not detected.

In this study case (i) and (ii) were analysed. After an inspection the probability of an assumed crack size  $a_n$  changes depending on the event of detection  $z$ . To link the probability of detecting a crack size  $a_n$  with occurring crack distributions (resulting from simulation) the Bayesian analysis according to Moan [12] was used. This model describes an equation for conditional probabilities, which gives the probability of event  $X$  given that event  $V$  is true for  $P(V) \neq 0$  [29].

$$P(X|V) = \frac{P(X) \cdot P(V|X)}{P(V)} \quad (7)$$

For case (i) the probability that a detected crack exists is given by  $P(a_n|z)$ . The probability of the occurrence of crack size  $a_n$  is given by  $P(a_n)$ .  $P(z|a_n)$  equals  $PoD(a_n)$  and is the probability that an existing crack of size  $a_n$  is detected (cf. Equation 6). Equation 9 shows  $P(z)$  over all occurring crack sizes  $a_n$  and their PoDs ( $P(z|a_n)$ ) according to Moan [12].

$$P(a_n|z) = \frac{P(a_n) \cdot P(z|a_n)}{P(z)} \tag{8}$$

$$P(z) = \sum_{k=a_{n,min}}^{k=a_{n,max}} \left( PoD(a_n)_k \cdot P(a_n)_k \right) \tag{9}$$

For case (ii) the probability of the existence of a non-detected crack  $P(a_n|\bar{z})$  is defined in Equation 10.  $P(\bar{z}|a_n)$  is the probability that an existing crack of size  $a_n$  is not detected. This equals  $1 - PoD(a_n)$ .  $P(\bar{z})$  is the probability for the event of no detection  $\bar{z}$ . According to Moan [12]  $P(\bar{z})$  is calculated by integration of  $1 - PoD(a)$  times the probability of a crack size  $a_n$ . Equation 11 shows the numerical integration over all occurring crack sizes  $a_n$  and their probability of not being detected.

$$P(a_n|\bar{z}) = \frac{P(a_n) \cdot P(\bar{z}|a_n)}{P(\bar{z})} \tag{10}$$

$$P(\bar{z}) = \sum_{k=a_{n,min}}^{k=a_{n,max}} \left( (1 - PoD(a_n)_k) \cdot P(a_n)_k \right) \tag{11}$$

Distributions were updated with both possible detection outcomes for an existing crack: case (i) (cf. Equation 8) and case (ii) (cf. Equation 10). Thus, crack size and RUL distributions after an inspection were analyzed (cf. Equation 5).

#### 4. Results and Discussion

##### 4.1. Crack size and RUL distribution after n years

The effect of linking crack size distribution with inspection outcome is shown in Figure 5(a). Resulting RUL distributions are illustrated in Figure 5(b). Distribution curves are plotted as histograms with a bin width of 0.01 mm for crack size and 3 years for RUL. Results without inspection are plotted in red lines. Updated distributions after an inspection are light grey for case (i) and dark grey for case (ii). Resulting values are listed in Table 3.

Table 3. Resulting median values of crack size  $a_n$  and RUL, standard deviation of RUL for the case without inspection and both cases with inspection.

Case Unit	Median value of crack size $a_n$ mm	Median value of RUL years	Standard deviation of RUL years
Without inspection	0.0458	78.41	445.68
Case (i): with crack detection	0.1949	33.27	46.95
Case (ii): without crack detection	0.0448	82.54	102.85

Crack sizes  $a_n$  without inspection after 20 years of operating time appear to be exponentially distributed. The most likely occurring crack sizes are smaller than 0.01 mm. The probability of occurrence strongly decreases with larger crack sizes. The distribution shape might result from the exponentially distributed initial crack size  $a_0$  which has a significant influence on the crack propagation. The median value of  $a_n$  is 0.0458 mm, which states that 50% of occurring crack sizes are smaller than 0.0458 mm. The median value of  $a_n$  increased from the initial crack size  $a_0$  by 34.5%.

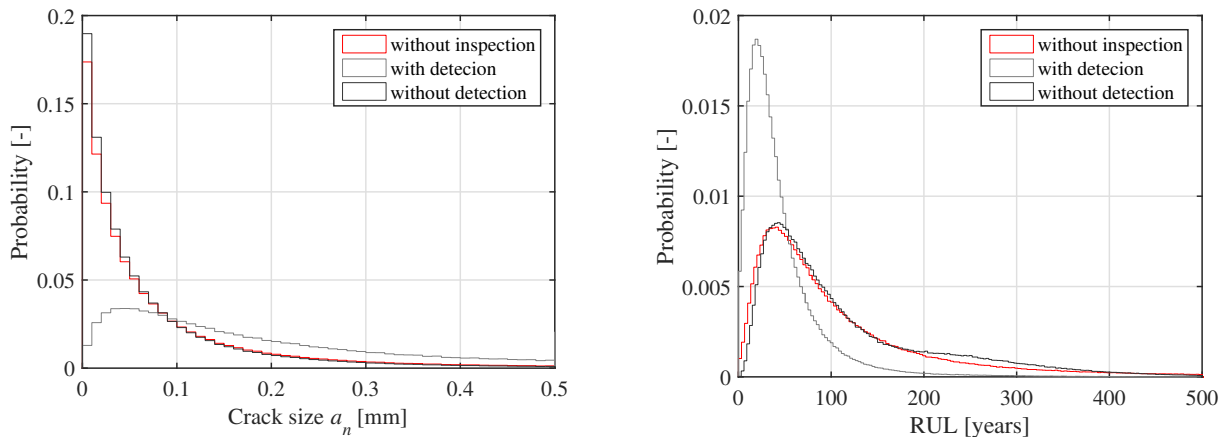


Fig. 5. (a) Probability of occurring crack size  $a_n$  with no inspection (red), and inspection with detection (light grey), inspection without detection (dark grey); (b) Probability of RUL with no inspection (red), and inspection with detection (light grey), inspection without detection (dark grey).

For the RUL distribution in the case of no inspection, a strong increase of probability until 39 years of RUL is shown, followed by a slow decrease. Median value of RUL results in 78 years. 90% of occurring RULs are higher than 24 years, whereas 10% of the values are above 280 years. Standard deviation is given by 446 years.

**Case (i):** In the case of inspection with crack detection the most likely bin occurs in between a crack size of 0.03 and 0.06 mm. The distribution is shaped by a wide covered spectrum, where a high number of crack sizes with small probabilities of occurrence are considered. Median crack size increased from initial crack size by 84.6% to a value of 0.1949 mm. The most likely RUL values occur between 30 and 40 years. The distribution increases strongly from zero to 18 years and decreases quickly after 21 years. RULs higher than 190 years occur with a probability approaching zero. The median RUL value is 33 years. 10% of occurring RULs are below 10 years. The standard deviation is 47 years.

**Case (ii):** In the case of not detecting a crack, the highest probability of occurrence is given for cracks smaller than 0.01 mm. Larger crack size bins have a strongly decreasing probability of occurrence. Median value is at 0.0448 mm. The increase is about 33% from initial crack size during 20 years of operation. 10% of crack sizes are nearly zero millimeters, whereas 90% are smaller than 0.21 mm. RUL values between 42 and 45 years occur most frequently. The distribution increases from zero to 42 years and slowly decreases after 45 years. RULs after 450 years occur rarely. Here, the probability of occurrence approaches zero percent. Median RUL value is 83 years. The standard deviation is equal to 103 years of RUL.

#### 4.2. Discussion

Results emerging from stochastic crack size analysis show, that the median crack value grows by 34.5% in 20 years, from a median value of initial crack size ( $a_0 = 0.03$  mm) to 0.0485 mm. RUL results in 78 years on average, but uncertainties are very high (standard deviation of 446 years). RULs over 500 years result from very small crack sizes (approaching zero). The failure rate of other OWT components (e.g. blades, gearbox, generator) can be approximately five times higher than the foundation failure rate [26]. Although these components can be exchanged, lifetime extension over several hundred years might be practically not feasible.

A limitation of the study is that Paris' Law was applied also for fatigue cracks with small initial size. Small cracks might propagate faster than calculated with Paris' Law [22]. This would result in an overestimation of the RUL. Therefore, care should be taken when interpreting the results. For a better estimation of the RUL, the analysis should distinguish between short and long cracks and apply suitable models for each situation separately.

The study shows that uncertainties are reduced when results from the stochastic crack propagation model are linked with inspection outcomes. The standard deviation of RUL estimation decreases strongly regardless of the inspection outcome. In case (i) the standard deviation is reduced by 89.5%, in case (ii) by 76.9%. These results suggest that inspections are mainly useful to eliminate the risk of large cracks in the structure.

For further reduction of uncertainty, it is recommended to either extend the inspection scope or introduce structural health monitoring. An extension can contain several inspections in succession or the integration of alternative inspection techniques (cf. Section 2.3.). Both approaches provide additional information about the integrity of the structure.

To address the question whether an inspection should be performed, costs and risk assessments are inevitable. Using structural health monitoring would prevent risks and costs of offshore operations, but might have to deal with other challenges, like data evaluation and equipment costs [27]. For a decision on lifetime extension, all components of the OWTs must be considered.

## 5. Conclusion and Outlook

Bayesian analysis was applied to link results from underwater inspections with a stochastic fatigue crack propagation model for monopile substructures of OWTs. Outcomes show a reduction of uncertainty in the estimation of the remaining fatigue life of these structures. These insights were obtained by comparing the shape of the distribution of various parameters (crack sizes, fatigue life) and its standard deviation. This is an important contribution to decrease risks in decision-making on lifetime extension of OWTs. On the other hand, underwater inspections imply a high health and safety risk for offshore workers and divers. Health and safety risk assessments are necessary in case of industrial implementation. This might question whether inspections are cost-efficient considering required effort and safety issues. Future works should address how the presented results can be integrated in a decision model for lifetime extension.

## Acknowledgements

This project has received funding from the European Unions Horizon 2020 research and innovation programme under the Marie Skłodowska-Curie grant agreement No 642108.



## References

- [1] DNV GL. Lifetime extension of wind turbines. Standard DNVGL-ST-0262; 2016.
- [2] Luengo MM & Kolios A. Failure Mode Identification and End of Life Scenarios of Offshore Wind Turbines: A Review. *Energies*, 8(8); 2015, DOI:10.3390/en8088339.
- [3] Faber T & Hansen K. First guideline for the continued operation of wind turbines. *Steel Construction - Design and Research Volume 3(1)*; 2010, p. 56-59. DOI: 10.1002/stco.201010008.
- [4] Ziegler L & Muskulus M. Comparing a fracture mechanics model to the SN-curve approach for jacket-supported offshore wind turbines: Challenges and opportunities for lifetime prediction. *ASME 2016 35th International Conference on Ocean, Offshore and Arctic Engineering Volume 6*; 2016, DOI: 10.1115/OMAE2016-54915.
- [5] Ziegler L, Schafhirt S, Scheu M & Muskulus M. Effect of Load Sequence and Weather Seasonality on Fatigue Crack Growth for Monopile-based Offshore Wind Turbines. *Energy Procedia* 94; 2016, p. 115-123.
- [6] DNV GL. Certification of lifetime extension of wind turbines. Service Specification DNVGL-SE-0263; 2016.
- [7] DNV GL. Probabilistic methods for planning of inspection for fatigue cracks in offshore structures. Recommended Practice DNVGL-RP-0001; 2015.
- [8] May P, Mendy G, Tallett P, Sanderson D & Sharp J. Structural integrity monitoring - Review and appraisal of current technologies for offshore applications. Research Report RR685. *Health and Safety Executive (HSE) Books*; 2009.
- [9] Bussièrès F, Montealegre F & Macdonald S. Offshore Wind Energy Operations and Maintenance Report. *Wind Energy Update (FC Business Intelligence)*; 2011.
- [10] ASNT. 2015. Homepage of The American Society of Nondestructive Testing. [www.asnt.org/MinorSiteSections/AboutASNT/Intro-to-NDT](http://www.asnt.org/MinorSiteSections/AboutASNT/Intro-to-NDT). Accessed on 04/30/2016.
- [11] NDT. 2014. Homepage of The Collaboration for NDT Education. [www.nde-ed.org/AboutNDT/aboutndt.htm](http://www.nde-ed.org/AboutNDT/aboutndt.htm). Accessed on 04/30/2016.
- [12] T. Moan. Updating of Reliability. *Structural Reliability Analysis*; 1996, p. 12.1-12.22.
- [13] Lotsberg I, Sigurdsson G, Fjeldstad A & Moan T. Probabilistic methods for planning of inspection for fatigue cracks in offshore structures. *Marine Structure* 46; 2016, p. 167-192.

- [14] Kallehave D, Byrne BW, LeBlanc Thilsted C & Kousgaard Mikkelsen K. Optimization of monopiles for offshore wind turbines. *Philosophical Transactions of The Royal Society A Mathematical Physical and Engineering Sciences* 373(2035); 2015, DOI: 10.1098/rsta.2014.0100.
- [15] Ziegler L & Muskulus M. Fatigue reassessment for lifetime extension of offshore wind monopile substructures. *Journal of Physics Conference Series* 753(9):092010; 2016, DOI: 10.1088/1742-6596/753/9/092010.
- [16] Ziegler L & Muskulus M. Lifetime Extension of Offshore Wind Monopiles: Assessment Process and Relevance of Fatigue Crack Inspection. *12th EAWE PhD Seminar on Wind Energy in Europe*, DTU Lyngby, Denmark; 2016.
- [17] Twidell J & Gaudiosi G. Offshore wind power. *Multi-Science Publishing Company Vol. 425*; 2009.
- [18] Stephens RI, Fatemi A, Stephens RR & Fuchs HO. *Metal fatigue in engineering*. 2nd ed. New York: John Wiley & Sons; 2000.
- [19] Paris P & Erdogan F. A critical analysis of crack propagation laws. *Journal of Basic Engineering, Trans. ASME* (85); 1963, p. 28-534.
- [20] Glaser B, Gubeljak N, Predan J, Gubeljak P & Veg A. Determination of calibration function for fatigue crack propagation by measurement surface deformation. *Sustainable Construction and Design*; 2013
- [21] Ciavarella M. Crack propagation laws corresponding to a generalized El Haddad Equation. *International Journal of Aerospace and Lightweight Structures Vol. 1, No. 1*; 2011, p. 109-118, DOI: 10.3850/S2010428611000109
- [22] Suresh S & Ritchie RO. Propagation of short fatigue cracks. *International Metals Reviews, Vol. 29, No.6*; 1984
- [23] Kirkemo F. Application of probabilistic fracture mechanics to offshore structures. *Applied Mechanics Reviews, 41(2)*; 1988, p. 61-84.
- [24] DNV. Design of Offshore Wind Turbine Structures. Offshore Standard DNV-OS-J101; 2014.
- [25] DNV GL. Fatigue design of offshore steel structures. Recommended Practice DNVGL-RP-0005; 2016.
- [26] Carroll J, McDonald A, Barrera Martin O, McMillan D & Bakhshi R. Offshore Wind Turbine Sub-Assembly Failure Rates Through Time. *EWEA Annual Conference and Exhibition 2015. European Wind Energy Association*; 2015, p. 112–116.
- [27] Kraemer P & Friedmann H. Vibration-based structural health monitoring for offshore wind turbines – Experimental validation of stochastic subspace algorithms. *Wind and Structures, Vol. 21, No. 6*; 2015, p. 693–707. DOI: <http://dx.doi.org/10.12989/was.2015.21.6.693>
- [28] Lotsberg I. *Fatigue Design of Marine Structures*. New York: Cambridge University Press; 2016.
- [29] Koch KR. *Einführung in die Bayes-Statistik*. Berlin: Springer-Verlag GmbH; 2000.
- [30] GL. Guideline for the Continued Operation of Wind Turbines. Guideline Germanischer Lloyd; 2009.
- [31] Maljaars J. Probabilistic fatigue life updating accounting for inspections of multiple critical locations. *International Journal of Fatigue Volume 68*; 2014, p. 24-37.
- [32] Jessen Nielsen J & Dalsgaard Sørensen J. On risk-based operation and maintenance of offshore wind turbine components. *Reliability Engineering & System Safety Volume 96(1)*; 2011, p. 218-229.